v. 5, n. 7, 2025

Journal of
Engineering
Research

Acceptance date: 25/07/2025

OpenFOAM AS A TOOL FOR ANALYZING CONJUGATE HEAT TRANSFER IN BUILDINGS

Edgard Elohim Canche Cauich
Ingeniero| Estudiante de Maestría en Energías Renovables y Eficiencia Energética
Universidad Autónoma de Campeche, Facultad de Ingeniería, Campus V, México

Felipe Noh Pat
Doctor | Profesor-Investigador
Universidad Autónoma de Campeche
Facultad de Ingeniería, Campus V, México
*Autor de correspondencia
felipnoh@uacam.mx

Jordy Alvarado Pacheco
Ingeniero| Estudiante de maestría en Energías Renovables y Eficiencia Energética
Universidad Autónoma de Campeche, Facultad de Ingeniería, Campus V, México

Miguel Ángel Gijón Rivera
Doctor | Profesor-Investigador
Tecnológico de Monterrey, Escuela de Ingeniería y Ciencias, México

Carlos Miguel Jiménez Xamán
Doctor | Profesor-Investigador
Universidad Autónoma de Campeche, Facultad de Ingeniería, Campus V, México

Mauricio Iván Huchin Miss
Doctor | Profesor-Investigador
Universidad Autónoma de Campeche, Facultad de Ingeniería, Campus V, México

Abstract: Global warming and more frequent heat waves, which are consequences of climate change, have driven research aimed at reducing heat gains in buildings. Since experimental evaluation of building components is often costly, computer simulations are frequently used to predict heat transfer to the indoor air of a building in greater detail and in an accessible way. This paper presents the verification and validation of three heat transfer cases representing building components and indoor air in buildings, using the free and open-source Computational Fluid Dynamics software OpenFOAM. The case studies considered include: natural convection in a square cavity with turbulent flow and surface radiative exchanges, conjugate heat transfer in a cavity with four solid walls, and conjugate heat transfer in a phase change material. The physical models are considered in two dimensions. The results obtained demonstrate that OpenFOAM is a tool capable of reproducing conjugate heat transfer phenomena in building systems with adequate accuracy, presenting overall relative errors of up to 10% compared to experimental results and numerical solutions reported in the literature. These findings position OpenFOAM as a viable and accessible option for future research in this field of study in Mexico.
Keywords: OpenFOAM, heat, buildings, validation, phase change material

INTRODUCTION

Buildings are systems that interact with external environmental conditions. In hot climates, heat gains into the indoor air are inevitable. However, in recent years, climate change has caused an increase in global temperatures and more frequent heat waves in countries such as India, Mexico, and Pakistan, which has led to a growing demand for electricity due to the intensive use of electromechanical systems for air conditioning, thus affecting the economy of the of middle-income households (International Energy Agency, 2024). In view of this problem, it is necessary to develop proposals that improve thermal comfort in buildings while reducing energy dependence and the environmental impact of conventional systems.

The experimental study of construction elements, passive systems, or eco-technologies that help reduce heat gain in buildings is often costly. A relatively low-cost alternative is simulation using Computational Fluid Dynamics (CFD). As a result of the exponential growth of computing technologies, it is now possible to obtain numerical solutions from complex mathematical models of fluid flow and heat transfer that are closer to reality.

In the field of CFD, there are users and code developers, the latter requiring advanced knowledge of physics, mathematics, and computing, as well as a considerable investment of time. The most common alternative when applying a case study is to be a user of CFD software. In this regard, commercial software packages are available, such as ANSYS Fluent, but the main disadvantage is that licenses can be expensive for research purposes. On the other hand, there are also free computational fluid simulation tools, such as Code_Saturne (EDF SA, 2021) and OpenFOAM (The OpenFOAM Foundation Ltd., n.d.).

OpenFOAM is a compendium of codes written in the C++ programming language. Its main drawback compared to commercial software is the lack of a free, user-friendly graphical interface, which means that it takes several months to learn. Furthermore, its application to conjugate heat transfer problems is even more complicated than in forced flow, especially due to the coupling between strongly linked equations (Tandis et al., 2025). Despite these disadvantages, its open-source nature makes it possible to modify the availa-

ble functions. For example, Välikangas (2016) improved a third-class boundary condition to allow for an accessible reading of ambient temperatures as a function of time. Piña et al. (2025), in Argentina, developed a diffuse--collimated radiation model for photothermal system and building simulations. Almaian &; Kastner (2025) concluded that OpenFOAM improves the design of energy-efficient buildings. Globally, the literature on OpenFOAM for conjugate heat transfer is scarce, but the versatility of the software is evident, and it is widely used in countries such as Sweden, India, and Argentina.

Figure 1 shows the main software and programming languages for CFD simulations applied to heat transfer in buildings. A total of 27 articles published by Mexican authors were reviewed. The most widely used commercial software is ANSYS Fluent, with 37.04%; on the other hand, Fortran is the most widely used language for developing proprietary codes, with 40.74%. The main elements modeled with proprietary codes are multiple-pane windows (Aguilar et al., 2015; Noh-Pat et al., 2020; Rodriguez-Ake et al., 2022), rooms with windows (Alvarez &&; Estrada, 2000; Olazo-Gómez et al., 2025), ventilated rooms (Serrano-Arellano et al., 2014), roofs with coatings (Hernández--Pérez, 2021), phase change materials (Xamán et al., 2020), solar chimneys (Zavala-Guillén et al., 2016), Trombe walls (Hernández-López et al., 2021), and ground-air heat exchangers (Aranda-Arizmendi et al., 2023). Recently, codes have been written in the C++ language (García-Pérez et al., 2023; Ríos-Arriola et al., 2023; Zavala-Guillén et al., 2025), and to a lesser extent in Matlab (Triano-Juárez et al., 2020) and Python (Canche-Cauich et al., 2024). Simplifications are adopted in the codes themselves, such as two-dimensional geometries, rectangular systems, and in some cases, transitional flow, due to the complexity of the physics and mathematics involved. On the other hand, ANSYS Fluent is popular because it has a graphical user interface and is capable of simulating complex three-dimensional geometries (Carreto-Hernandez et al., 2024; Contreras-Aguilar et al., 2025; Díaz--Calderón et al., 2021; Díaz-Hernández et al., 2017; Hernández-Castillo et al., 2022; Hinojosa et al., 2016; Maytorena et al., 2023; Navarro et al., 2021; Ordóñez, 2019; Piña-Ortiz et al., 2018). Regarding OpenFOAM, authors Noh--Pat et al. (2024) modeled concrete hollow blocks with phase change material (PCM) for a period of two days under warm, subhumid conditions in the city of Mérida.

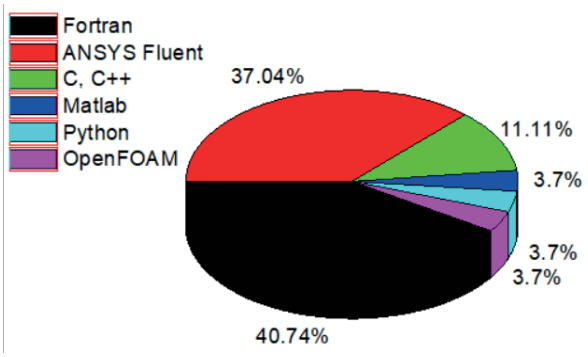

Figure 1. Computational tools and programming languages used in Mexico for CFD simulations of heat transfer in buildings.

Due to OpenFOAM's ability to model complex geometries and physics, as well as its open source and free code, this paper presents the validations and verifications of three representative heat transfer cases involving building components and indoor air: natural convection with turbulent flow and radiative exchanges in a square cavity filled with air, conjugate heat transfer in a cavity with four solid walls, and conjugate heat transfer in a PCM.

METHODOLOGY.

A CFD-based study is structured in three phases: pre-processing, processing, and post--processing. **Figure 2** illustrates this process. Pre-processing requires about 70% of the

user's time, mainly due to the spatial discretization of the physical model representing the real system into a set of non-overlapping control cells or volumes, i.e., the generation of the computational mesh. In addition, this phase involves compiling physical properties and selecting and configuring boundary and initial conditions, the turbulence model, numerical schemes, and iterative matrix solvers. The mesh quality test verifies the non--orthogonality, obliquity, and aspect ratio of the cells (Greenshields &; Weller, 2022). Processing consists of the numerical solution of mathematical models, formulated as partial differential equations, where the Finite Volume Method (FVM) is usually applied (Xamán &; Gijón-Rivera, 2016). The study of spatial mesh independence consists of reducing the size of the cells and, if the phenomenon is transient, also the time step, in order to improve the consistency of the results. Finally, post-processing is the analysis of the results. Validation is the comparison of the numerical results with those of an experiment or, in the absence of an experiment, with the numerical solutions of other authors. This is an important step because it ensures that the CFD models can adequately approximate reality and that the user is using them correctly.

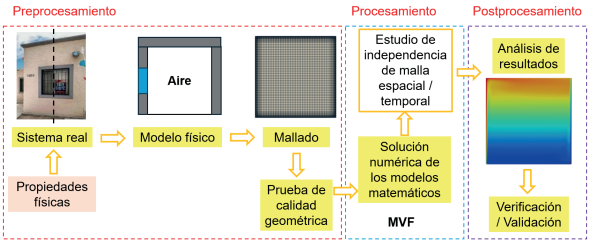

Figure 2. Stages of a CFD study.

DESCRIPTION OF THE CASE STUDIES

CASE 1: NATURAL CONVECTION WITH TURBULENT FLOW IN A SQUARE CAVITY FILLED WITH AIR.

The phenomenon is considered in a steady state and in two dimensions. The physical models for case 1, without radiation exchange (case C1a) and with radiation exchange (case C1b), are shown in **Figure 3**. The model consists of a closed square cavity containing air, with dimensions of 0.75 x 0.75 m. The Rayleigh number (Ra) for this case is $1.58x10^{9}$ [9] turbulent flow is generally assumed when the Ra number is greater than $1x10^{6}$ [6] (Barakos et al., 1994).

The boundary conditions that solve the mathematical models are shown in Figure 3, where the horizontal walls of the cavity are adiabatic, while the left vertical wall is given a constant temperature T_H , and the right vertical wall is given a constant temperature T_C . The air rises near the warmer wall and descends near the colder wall as a result of density variations. The boundary conditions for the velocity field (U) are the no-slip conditions caused by the viscosity of the air, which means that the velocity components u and v in the x and y directions, respectively, are equal to 0 m/s at the solid walls of the cavity. All thermal properties of air are evaluated at the average temperature between the hot temperature ($T_{H)}$)and cold temperature ($T_{C)}$).

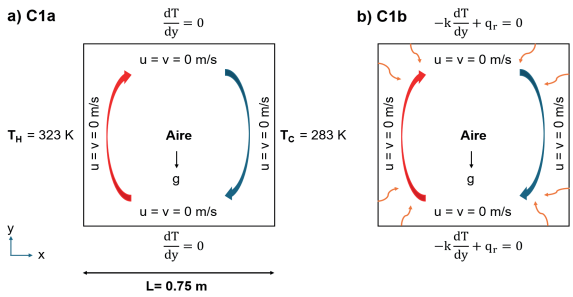

Figure 3. Physical models of case 1 a) without surface radiative exchanges (C1a) and b) with radiative exchanges (C1b).

In this study, RANS (*Reynolds-Averaged Navier-Stokes equations*) turbulence models of two equations were analyzed: k-ω-SST and buoyant k-ε. The initial conditions for turbulent kinetic energies (k) were set to small values, while turbulent dissipation kinetic

energies (ε and ω) were set to very large values. Low Reynolds number wall functions were set as boundary conditions, and the viscous layer (y+ < 5) was resolved (WoldDynamics, 2021).

With regard to radiative exchanges (q_r), the emissivity of the interior surfaces was considered to be equal to 0.3, in accordance with the authors Vijaya Kumar et al. (2020), this value corresponds to mild steel.

CASE 2: CONJUGATE HEAT TRANSFER IN A CAVITY WITH FOUR SOLID WALLS.

The phenomenon is considered in a steady state and in two dimensions. The physical model of case 2 is shown in **Figure 4**. It is a square cavity whose dimensions L and W_A are a function of the Ra number, defined according to **equation 1**:

$$Ra = \frac{g\beta(T_H - T_C)L^3}{\upsilon^2}Pr \qquad (1)$$

In this case, Ra values equal to $1x10^1$, $1x10^3$, $1x10^4$, and $1x10^6$ were analyzed. The W_A dimension was calculated according to **equation 2** (Zhao et al., 2007):

$$\cos(37°) = \frac{W_A}{L} \qquad (2)$$

Constant temperatures T_H and T_C are fixed on the vertical walls of the cavity. At the solid-air interfaces, the continuity of heat transfer by conduction must be satisfied. This coupling between the solid (S) and air equations increases the difficulty of the numerical solution. The thermal conductivity of the solid is 0.0263 W/m·K (Zhao et al., 2007).

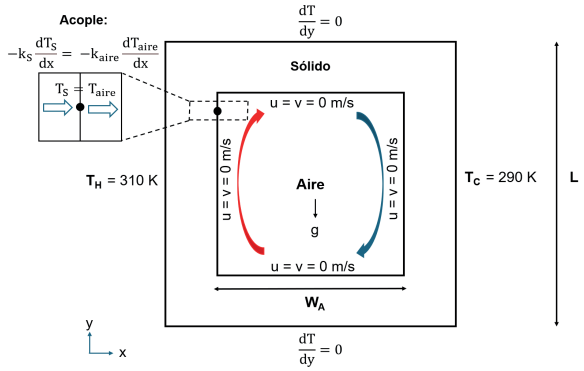

Figure 4. Physical model of case 2.

CASE 3: CONJUGATE HEAT TRANSFER IN A PCM.

The phenomenon is considered in a transient state and in two dimensions. The physical model of case 3 is shown in **Figure 5**. It is a square cavity filled with air with dimensions of 10 x 10 cm, on whose right wall there is a PCM container with a thickness of 1 cm. Initially, the PCM is in the liquid phase at a temperature significantly higher than that of the adjacent air, which causes the release of thermal energy stored during the melting process. The objective of this case is to simulate the effect of PCM solidification on natural convection in laminar flow (Labihi et al., 2017).

The initial temperature condition for the air is approximately 311 K, and for the PCM it is 333.2 K. In this work, the melting of the PCM was first simulated according to the data of Labihi et al. (2017).

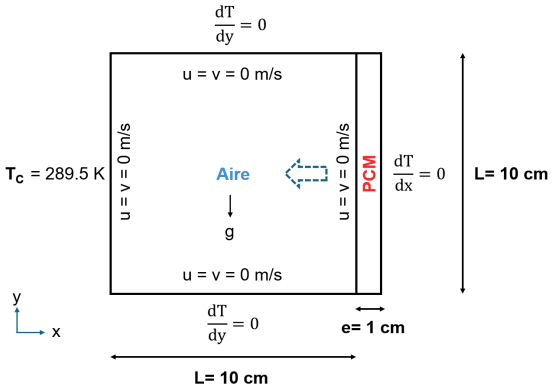

Figure 5. Physical model of case 3.

The thermal properties of PCM are shown in **Table 1**. It is PCM60, which is a carboxylic acid type and is marketed by *Kaplan Energy* (Labihi et al., 2017). The PCM simulation in OpenFOAM was carried out using the average thermal properties between the liquid and solid phases, represented by the subscripts l and s, respectively.

MATHEMATICAL MODELS

The equations governing the phenomena of motion and heat transfer in a fluid are called Navier-Stokes equations, which express physical principles of conservation. Considering turbulent flow in a transient state, the equations are (Greenshields &; Weller, 2022):

Mass conservation equation.

$$\frac{\partial \rho}{\partial t} + \nabla \cdot (\rho U) = 0 \quad (3)$$

Momentum conservation equation.

$$\frac{\partial(\rho U)}{\partial t} + \nabla \cdot (\rho U \otimes U) = \nabla \cdot \bar{\tau} - \nabla p + \rho g \quad (4)$$

Viscous stress tensor.

$$\bar{\tau} = 2\mu_{eff}\,[(\nabla U) + (\nabla U)^T] \; - \frac{2}{3}\mu_{eff}(\nabla \cdot U)I \quad (5)$$

Effective viscosity.

$$\mu_{eff} = \mu + \mu_t \quad (6)$$

Dynamic viscosity.

$$\mu = \rho \upsilon \quad (7)$$

Turbulent dynamic viscosity.

$$\mu_t = \rho \upsilon_t \quad (8)$$

Energy conservation equation.

$$\frac{\partial(\rho h)}{\partial t} + \nabla \cdot (\rho U h) + \frac{\partial\left(\rho \frac{1}{2}|U|^2\right)}{\partial t} - \frac{dp}{dt} = -\nabla \cdot \left(\rho U \frac{1}{2}|U|^2\right) + \nabla \cdot (\alpha_{eff} \nabla h) + \rho(U \cdot g) + \nabla \cdot [\bar{\tau} \cdot U] \quad (9)$$

Effective thermal diffusivity.

$$\alpha_{eff} = \frac{\mu}{Pr} + \frac{\mu_t}{Pr_t} \quad (10)$$

The total energy equation is solved to obtain the enthalpy (h). The temperature field is calculated from the relationship between enthalpy and temperature, which is expressed in Equation 11:

$$dh = C_p dT \quad (11)$$

Variations in air density as a result of temperature fluctuations are modeled using the ideal gas equation of state, according to Equation 12:

$$\rho = \frac{p}{RT} \quad (12)$$

Turbulence is simulated using two-equation RANS models. These turbulence models evaluate turbulent eddy viscosity (υ_t), closing the momentum and energy equations.

For the solid regions and PCM, only the heat conduction equation is solved, which is presented in Equation 13. The temperature field is determined as in Equation 11.

$$\frac{\partial(\rho h)}{\partial t} = \nabla \cdot \left(\frac{k}{C_p} \nabla h\right) \quad (13)$$

The enthalpy method available in OpenFOAM is used for phase change. Phase change is taken into account in the term h, which is the sum of the contribution from sensible heat (C_p T) and latent heat (Δh):

$$h = C_p T + \Delta h \quad (14)$$

Latent heat depends on the temperature of the solid (T_s) and liquid (T_l), as well as the liquid fraction (f):

$$\Delta h = f(T) = \begin{cases} \Delta h & T \geq T_l \\ \Delta h \cdot f & T_l > T \geq T_s \\ 0 & T < T_s \end{cases} \quad (15)$$

Surface radiative exchanges are modeled using the view factor method available in OpenFOAM, which is based on the net radiation method, which consists of performing an energy balance q_r for element k at location r on each wall, assuming that it is isothermal, gray, and diffuse. Radiance ($q_{o)}$)is the sum of the radiation emitted and reflected by element k, while irradiance (q_i) is the sum of the contributions of elements k' on element k. There-

Phase change temperatures (°C)	ρ_l (kg/m$^{(3)}$)	ρ_S ($^{kg/m^3}$)	C_S (J/kg· K)	C_l (J/kg· K)	k_S (W/m· K)	k_l (W/m· K)	Δh (J/kg)
49	580	694	170	1750	0.2	0.2	137000

Table 1. Thermal properties of PCM (Labihi et al., 2017).

Cases	Spatial independence	Temporal independence
	90 x 90 grid	Stationary
2	68 x 68 mesh (air + solid)	Stationary
3	100 x 100 mesh (air + PCM)	1 s

Table 2. Spatial and temporal grid independence.

Ampofo and Karayiannis (2003)	Vijaya Kumar et al. (2020)	**Error (%)**	**Present study k-ω-SST**	**Error (%)**	**Present study Buoyant k-ε**	**Error (%)**
65.	59.0	9.9	58.79	10.29	59.14	9.76

Table 3. Average Nusselt number on the hot wall (C1a).

Ra	(Zhao et al., 2007)	(García-Pérez et al., 2023)	**Present study**	**Error (%)** Zhao et al.	**Error (%)** García-Pérez et al.
10^1	1	1.0	1.0	0.00	0.00
10^3	1.02	1.02	1.02	0.28	0.28
10^4	1.41	1.39	1.37	3.19	1.80
10^6	2.90	2.85	2.77	4.41	2.74

Note: Relative percentage errors.

Table 4. Verification of case 2.

fore, the resulting energy balance is:

$$q_r(r_k) = q_o(r_k) + q_i(r_k) \quad (16)$$

Radiosity.

$$q_o(r_k) =* \varepsilon_k \sigma T^4(r_k) + \varrho_k^* q_i(r_k) \quad (17)$$

Irradiance.

$$q_i(r_k) = \int_{A_k} q_o(r_k') dF_{dA_k - dA_k'} \quad (18)$$

NUMERICAL SOLUTION

The differential equations presented above were solved in OpenFOAM using the MVF because the physical principles of conservation are guaranteed during the integration of the equations. This method starts by expressing the volume integrals in each cell of the discretized space as area integrals. To evaluate these area integrals, information is required on the faces of the cells. Since this information is initially unknown, a numerical interpolation scheme is applied for each mathematical term. After selecting the numerical discretization scheme, a set of algebraic equations is obtained that must be solved with an iterative matrix solver. The boundary and initial conditions are also discretized and added to the matrix of each scalar and vector field.

The meshes were generated with the OpenFOAM blockMesh tool, which is a code where the rectangular coordinates of the vertices

of the geometry are written. Non-uniform meshes were generated, with finer cells near the walls because temperature and velocity gradients occur in these areas. **Table 2** summarizes the spatial and temporal mesh independence for the case studies. In the transient PCM case, a time step of 1 s was set.

The convective terms of the mathematical models were discretized using the first-order upwind numerical scheme due to the relatively low speeds of natural convection and its good numerical stability. The diffusive terms were discretized using the second-order centered scheme , and the time term of the heat conduction equation with phase change was discretized using the first-order implicit Euler scheme.

The chtMultiRegionFOAM solver was used and the post-processing functions were configured: wallHeatFlux, to record heat flows due to convection; and probes, to record point values of temperatures in the case of PCM.

RESULTS AND DISCUSSIONS.

In the first two cases, the Nusselt number (Nu) was calculated, a dimensionless number that expresses the ratio between heat transfer by natural convection and heat transfer by reference conduction, defined in **equation 19**.

$$Nu = \frac{\dot{q}_{conv}}{\dot{q}_{cond}} = \frac{wallHeatFlux_{OpenFOAM}}{k\left(\frac{T_H - T_C}{L}\right)} \qquad (19)$$

CASE 1: NATURAL CONVECTION WITH TURBULENT FLOW IN A SQUARE CAVITY FILLED WITH AIR.

Table 3 shows the validation of case C1a by comparing the average Nusselt number on the hot vertical wall of the cavity with experimental results from the authors of the case, Ampofo & Karayiannis (2003), and numerical simulations by Vijaya Kumar et al. (2020) in OpenFOAM.

The authors Vijaya Kumar et al. (2020) modified the k-ω-SST turbulence model to add the turbulent production and dissipation equations due to buoyancy. However, when comparing the results of this study with the standard k-ω-SST model, the relative percentage error only decreased by 0.31%; and compared to the buoyant k-ε model, which considers turbulent buoyancy effects, the result did not improve. Vijaya Kumar et al. (2020) concluded that the added terms are not always significant, but they will be when density gradients are additionally influenced by species mass concentration gradients, for example.

In this study, the buoyant k-ε model performed better than the standard k-ω-SST model, but with practically negligible differences. The buoyant k-ε model applied, like other models in the k-ε family, has the disadvantage of being very sensitive to mesh resolution near walls, making it difficult to find consistent numerical solutions (Versteeg & Malalasekera, 2007). The errors in this study can be attributed to multiple factors, such as the mathematical formulations, the adiabatic conditions on the horizontal walls, which are difficult to achieve in real life, and the fact that the flow in the cavity is perhaps not completely turbulent, but rather in transition.

Figure 6 shows the validation of case C1b, comparing the temperature results on the central vertical line of the cavity. The emissivity value suggested by Vijaya Kumar et al. (2020) , was usedalthough the exact value is not known. However, the figure shows that the k-ω-SST model with radiative exchanges (C1b) provides results that are equal to the k-ω-SST model with turbulent buoyancy effects and radiation exchanges . It can be seen that the buoyant k-ε model with radiation (C1b) approximated the experimental results of Ampofo and Karayiannis (2003) , better in the center of the cavitybut with pronounced differences near the horizontal walls. As indicated by Vijaya Kumar et al. (2020), when radiation is considered, the overall heat trans-

fer increases and the Nu number is overestimated: convective heat transfer decreases and the contribution from radiation represents around 34% at the hot wall. These results are for validation and verification purposes only. In addition, the results of turbulence models without radiative exchanges (cases C1a) are presented to illustrate the effect.

The reason why models with radiation (cases C1b) better approximate the experimental results than models without radiation (cases C1a) is due to the boundary condition on the horizontal walls. When radiation is considered, a non-uniform temperature pattern arises that is not reproduced under ideal adiabatic conditions.

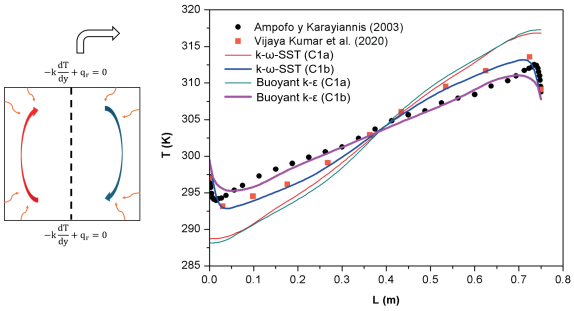

Figure 6. Validation of case C1b.

CASE 2: CONJUGATE HEAT TRANSFER IN A CAVITY WITH FOUR SOLID WALLS.

Table 4 shows the verification of case 2 by comparing the global Nu numbers obtained with OpenFOAM with those of the authors of the reference problem, Zhao et al. (2007), and those of García-Pérez et al. (2023), who solved the case with their own code written in the C language.

As the Ra number increases, so does the Nu number. This behavior is expected, as the flow becomes more convective and transitions to turbulence. The relative percentage error increases to 4.41% for a Ra of $1x10^6$ when compared to the result of Zhao et al. (2007). Regarding the result of García-Pérez et al. (2023), the maximum error is 2.74% for this same Ra number.

CASE 3: CONJUGATE HEAT TRANSFER IN A PCM

Figure 7 shows the results of the simulation of the PCM solidification phenomenon. At time t=30 s, it can be seen that the PCM is in the liquid phase (f=1) and only a small proportion located at the bottom is in the solid phase (f=0). The PCM begins to release the stored thermal energy into the adjacent air during melting; as a result, vortices arise in the center of the cavity, velocity gradients are concentrated near the walls, and the thickness of the hydrodynamic layer is thin. These characteristics indicate that natural convection heat transfer is effective and dominant. The behavior described above continues throughout the phase change, demonstrating the PCM's ability to regulate internal conditions.

At time t= 3690 s, the pasty region in the PCM is visible, where the liquid and solid phases coexist simultaneously. At time t= 9030 s, a minimal fraction of liquid (f=0.8) remains in the upper part of the PCM, solidification is nearing completion, and heat transfer by convection decreases, which is why the central vortices have also decreased.

Finally, at time t= 36000 s, solidification is complete and a steady state is reached. A central vortex is evident, as is an increase in the thickness of the hydrodynamic layer, in which the velocities are much lower due to the decrease in thermal energy supplied by the PCM. The characteristics described are common in natural convection at low Ra numbers (Barakos et al., 1994; Oyewola et al., 2021).

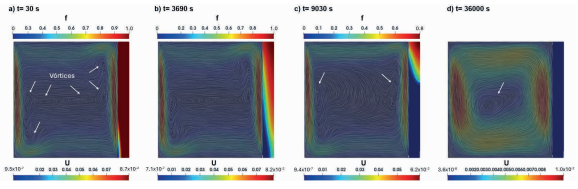

Figure 7. Transient evolution of the phase change: a) t= 30 s (start of solidification), b) t= 3690 s (solidification), c) t= 9030 s (end of solidification) and d) t= 36000 s (stable state).

Figure 8 shows the validation of the case by comparing the results of the temporal evolution of the temperatures, which were recorded using the probes function at the central points of the cavity and the PCM. The simulated phase change process took approximately two hours the experimental results of Labihi et al. (2017) indicate that this process is actually much faster. The maximum percentage error obtained in the present study was 11.63% and was recorded during the end of solidification, at approximately 2 hours and 9 minutes. The numerical results of the authors García-Pérez et al. (2023) with their own code behaved similarly to the present study, with a maximum error of 10.58%. Labihi et al. (2017) modified their numerical code to consider the actual change in PCM density. In the present study, the PCM density was considered constant and equal to the average value between the liquid and solid phases, which is the reason for the maximum error.

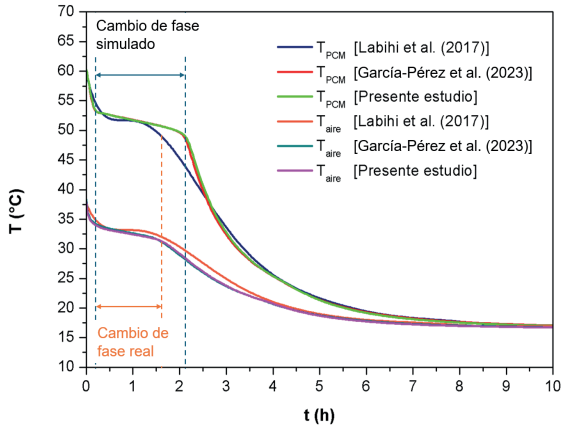

Figure 8. Validation of case 3.

CONCLUSIONS

The validations and verifications of three heat transfer cases representative of building elements were presented using the free and open-source CFD software OpenFOAM.

The standard k-ω-SST turbulence model provided results similar to the buoyant k-ε model, so it is concluded that the turbulent production and dissipation terms caused by buoyancy are insignificant in this case. In addition, during the spatial independence process, it was observed that the models are sensitive near the walls, unlike in the center of the cavity. Conjugate heat transfer problems are more complex, and computation time increases due to the coupling between the equations. Finally, it is concluded that OpenFOAM is capable of providing reliable results in the area of heat transfer. As it is a tool that is not widely used in Mexico, its use is recommended in this field of research to propose strategies that help reduce heat gains in buildings, including PCM in the envelope.

NOMENCLATURE

C	Specific heat (J/kg·K)	α	Thermal diffusivity (m^2 /s)
Δh	Latent heat (J/kg)	β	Expansion coefficient (1/K)
F	Liquid fraction	ε, ω	Turbulent dissipation energies (m^2 /s^3)
F	View factor	*ε	Emissivity
g	Gravity (9.81 m/s^2)	μ	Dynamic viscosity (kg/m·s)
h	Enthalpy (J/kg)	υ	Kinematic viscosity (m^2 /s)
K	Thermal conductivity (W/m·K), turbulent kinetic energy (m^2 /s^2)	ρ	Density (kg/m^3)
L	Characteristic length (m)	ϱ	Reflectivity
Un	Nusselt number	σ	Stefan Boltzmann constant ($5.67x10^{-8}$ W/m^4·K)
P	Pressure (Pa)		Viscous stress tensor
Pr	Prandtl number	Abbreviations	
q_r	Radiative exchange	CFD	Computational Fluid Dynamics
R	Ideal gas constant (J/kg·K)	MVF	Finite Volume Method
Ra	Rayleigh number	PCM	Phase Change Material
T	Time (s, h)	Subscripts	
T	Temperature (°C, K)	eff	Effective
U	Velocity field (m/s)	S, l	Solid, liquid
Greek letters		t	Turbulent

REFERENCES

Aguilar, J. O., Xaman, J., Álvarez, G., Hernández-Pérez, I., & López-Mata, C. (2015). Thermal performance of a double pane window using glazing available on the Mexican market. Renewable Energy, 81, 785–794. https://doi.org/10.1016/j.renene.2015.03.063

Almaian, M., & Kastner, P. (2025). 3D Heat Transfer Analysis in Architectural Modeling: A Case Study with OpenFOAM (pp. 561–568). https://doi.org/10.1007/978-981-97-8305-2_79

Alvarez, G., & Estrada, C. A. (2000). Numerical heat transfer in a cavity with a solar control coating deposited to a vertical semitransparent wall. International Journal for Numerical Methods in Fluids, 34(7), 585–607. https://doi.org/10.1002/1097-0363(20001215)34:7<585::AID-FLD72>3.0.CO;2-M

Ampofo, F., & Karayiannis, T. G. (2003). Experimental benchmark data for turbulent natural convection in an air filled square cavity. International Journal of Heat and Mass Transfer, 46(19). https://doi.org/10.1016/S0017-9310(03)00147-9

ANSYS. (s/f). ANSYS Fluent. Recuperado el 19 de junio de 2025, de https://www.ansys.com/products/fluids/ansys-fluent

Aranda-Arizmendi, A., Rodríguez-Vázquez, M., Jiménez-Xamán, C. M., Romero, R. J., & Montiel-González, M. (2023). Parametric Study of the Ground-Air Heat Exchanger (GAHE): Effect of Burial Depth and Insulation Length. Fluids, 8(2), 40. https://doi.org/10.3390/fluids8020040

Barakos, G., Mitsoulis, E., & Assimacopoulos, D. (1994). Natural convection flow in a square cavity revisited: Laminar and turbulent models with wall functions. International Journal for Numerical Methods in Fluids, 18(7), 695–719. https://doi.org/10.1002/fld.1650180705

Canche-Cauich, E. E., Noh-Pat, F., Jiménez-Torres, M. A., Lezama-Zárraga, F. R., & Cortazar-Miranda, B. (2024). Efecto de la conducción de calor en una ventana de vidrio doble. Memorias XXI Congreso Internacional, XXVII Congreso Nacional de Ciencias Ambientales y VIII Iberoamericano de Física y Química Ambiental. Revista Internacional de Contaminación Ambiental, 40. https://doi.org/10.20937/RICA.2024.40.ANCA

Carreto-Hernandez, L. G., Moya, S. L., Varela-Boydo, C. A., Juárez Sosa, I., Báez-García, W. G., Reyes, V. A., & Morales, J. M. (2024). Analysis of natural convection in a representative cavity of a room considering oscillatory boundary conditions: An experimental and numerical approach. International Journal of Thermal Sciences, 206, 109357. https://doi.org/10.1016/j.ijthermalsci.2024.109357

Contreras-Aguilar, J. A., Gijón-Rivera, M., Rivera-Solorio, C. I., & Noh-Pat, F. (2025). Thermo-economic assessment of a double-layer phase-change material in building roofs in a semi-arid climate. Thermal Science and Engineering Progress, 57, 103093. https://doi.org/10.1016/j.tsep.2024.103093

Díaz-Calderón, S. F., Castillo, J. A., & Huelsz, G. (2021). Indoor air quality evaluation in naturally cross-ventilated buildings for education using age of air. Journal of Physics: Conference Series, 2069(1), 012182. https://doi.org/10.1088/1742-6596/2069/1/012182

Díaz-Hernández, H., Aguilar-Castro, K., Macías-Melo, E., & Serrano-Arrellano. (2017). Diseño de un intercambiador de calor tierra-aire en clima cálido-húmedo. Revista del Desarrollo Tecnológico, 1, 44–51.

EDF SA. (2021). Code_Saturne. https://www.code-saturne.org/cms/web/

García-Pérez, D., Xamán, J., Zavala-Guillén, I., Chávez-Chena, Y., Simá, E., & Arce, J. (2023). Annual evaluation of a modified wall with PCM to reduce energy consumption and CO2 emissions in Southeast Mexico. Energy and Buildings, 292. https://doi.org/10.1016/j.enbuild.2023.113129

Greenshields, C. J., & Weller, H. G. (2022). Notes on Computational Fluid Dynamics: General Principles. CFD Direct Ltd.

Hernández-Castillo, P., Castillo, J. A., & Huelsz, G. (2022). Heat transfer by natural convection and radiation in three dimensional differentially heated tall cavities. Case Studies in Thermal Engineering, 40, 102529. https://doi.org/10.1016/j.csite.2022.102529

Hernández-López, I., Vázquez-Beltrán, E., Xamán, J., Chávez, Y., Hinojosa, J. F., & Noh-Pat, F. (2021). Heating potential prediction of a trombe wall system under temperate climate conditions of Mexico: Case of Cwa-Cwb Köppen classification. Journal of Building Engineering, 44, 103308. https://doi.org/10.1016/j.jobe.2021.103308

Hernández-Pérez, I. (2021). Influence of Traditional and Solar Reflective Coatings on the Heat Transfer of Building Roofs in Mexico. Applied Sciences, 11(7), 3263. https://doi.org/10.3390/app11073263

Hinojosa, J., Rodríguez, N., & Xamán, J. (2016). Heat transfer and airflow study of turbulent mixed convection in a ventilated cavity. Journal of Building Physics, 40(3), 204–234. https://doi.org/10.1177/1744259115611640

International Energy Agency. (2024). Electricity Mid-Year Update. https://iea.blob.core.windows.net/assets/d114506a-f-741-4264-90aa-d476f79eb83e/ElectricityMid-YearUpdate_July2024.pdf

Labihi, A., Aitlahbib, F., Chehouani, H., Benhamou, B., Ouikhalfan, M., Croitoru, C., & Nastase, I. (2017). Effect of phase change material wall on natural convection heat transfer inside an air filled enclosure. Applied Thermal Engineering, 126. https://doi.org/10.1016/j.applthermaleng.2017.07.112

Maytorena, V. M., Hinojosa, J. F., Moreno, S., & Buentello-Montoya, D. A. (2023). Thermal performance analysis of a passive hybrid earth-to-air heat exchanger for cooling rooms at Mexican desert climate. Case Studies in Thermal Engineering, 41, 102590. https://doi.org/10.1016/j.csite.2022.102590

Navarro, J. M. A., Hinojosa, J. F., & Piña-Ortiz, A. (2021). Computational fluid dynamics and experimental study of turbulent natural convection coupled with surface thermal radiation in a cubic open cavity. International Journal of Mechanical Sciences, 198, 106360. https://doi.org/10.1016/j.ijmecsci.2021.106360

Noh-Pat, F., Gijón-Rivera, M., Xamán, J., Zavala-Guillén, I., Aguilar, J. O., & Rodríguez-Pérez, M. (2020). Modelling of an energy-efficient open double-glazing unit for the main climatic conditions of Mexico. Indoor and Built Environment, 29(5), 746–764. https://doi.org/10.1177/1420326X19862601

Noh-Pat, F., Gijón-Rivera, M., Zavala-Guillén, I., Rivera-Solorio, C. I., May-Tzuc, O., & Shih, M. Y. (2024). Thermo-energy performance of a phase change material integrated into lightweight hollow concrete roofs in warm–subhumid climate. Energy and Buildings, 312, 114213. https://doi.org/10.1016/j.enbuild.2024.114213

Olazo-Gómez, Y., Hernández-López, I., Zavala-Guillén, I., Hernández-Pérez, I., & García-Pérez, D. (2025). Numerical study of a cool roof and double-glazing window coupled to an air-cavity under a tropical Mexican climate. Case Studies in Thermal Engineering, 73, 106372. https://doi.org/10.1016/j.csite.2025.106372

Ordóñez, M. (2019). Los intercambiadores de calor tierra-aire en el Karst de Yucatán: un estudio de viabilidad. Centro de Investigación Científica de Yucatán.

Oyewola, O. M., Afolabi, S. I., & Ismail, O. S. (2021). Numerical simulation of natural convection in rectangular cavities with different aspect ratios. Frontiers in Heat and Mass Transfer, 17(1), 1–8. https://doi.org/10.5098/HMT.17.11

Piña, J. S., Catalano, J. C., Cortizo, M. C., Venier, C. M., Pairetti, C. I., Corzo, S. F., Godino, D., & Ramajo, D. (2025). Development of a boundary-coupled CFD model for collimated-diffusive radiation. International Journal of Heat and Mass Transfer, 248, 127170. https://doi.org/10.1016/j.ijheatmasstransfer.2025.127170

Piña-Ortiz, A., Hinojosa, J. F., Xamán, J. P., & Navarro, J. M. A. (2018). Test of turbulence models for heat transfer within a ventilated cavity with and without an internal heat source. International Communications in Heat and Mass Transfer, 94, 106–114. https://doi.org/10.1016/j.icheatmasstransfer.2018.03.021

Ríos-Arriola, J., Gómez-Arias, E., Zavala-Guillén, I., Velázquez-Limón, N., Bojórquez-Morales, G., & López-Velázquez, J. E. (2023). Numerical modeling of soil temperature variation under an extreme desert climate. Geothermics, 112. https://doi.org/10.1016/j.geothermics.2023.102731

Rodriguez-Ake, A., Xamán, J., Hernández-López, I., Sauceda, D., Carranza-Chávez, F. J., & Zavala-Guillén, I. (2022). Numerical study and thermal evaluation of a triple glass window under Mexican warm climate conditions. Energy, 239, 122075. https://doi.org/10.1016/j.energy.2021.122075

Serrano-Arellano, J., Gijón-Rivera, M., Riesco-Ávila, J. M., Xamán, J., & Álvarez, G. (2014). Numerical investigation of transient heat and mass transfer by natural convection in a ventilated cavity: Outlet air gap located close to heat source. International Journal of Heat and Mass Transfer, 76, 268–278. https://doi.org/10.1016/j.ijheatmasstransfer.2014.04.055

Tandis, E., Cardiff, P., & Ashrafizadeh, A. (2025). Analysis of Coupling Strategies for Conjugate Heat Transfer Problems. OpenFOAM® Journal, 5, 38–58. https://doi.org/10.51560/ofj.v5.92

The OpenFOAM Foundation Ltd. (s/f). OpenFOAM. Recuperado el 19 de junio de 2025, de https://openfoam.org/

Triano-Juárez, J., Macias-Melo, E. V., Hernández-Pérez, I., Aguilar-Castro, K. M., & Xamán, J. (2020). Thermal behavior of a phase change material in a building roof with and without reflective coating in a warm humid zone. Journal of Building Engineering, 32, 101648. https://doi.org/10.1016/j.jobe.2020.101648

Välikangas, T. (2016). Conjugate heat transfer in OpenFOAM. In Proceedings of CFD with OpenSource software, 2016, edited by Nilsson. H. https://www.tfd.chalmers.se/~hani/kurser/OS_CFD_2016/

Versteeg, H., & Malalasekera, W. (2007). An Introduction To Computacional Fluid Dynamics (Second edition). Pearson Education Limited 1995.

Vijaya Kumar, G., Kampili, M., Kelm, S., Arul Prakash, K., & Allelein, H.-J. (2020). CFD modelling of buoyancy driven flows in enclosures with relevance to nuclear reactor safety. Nuclear Engineering and Design, 365, 110682. https://doi.org/10.1016/j.nucengdes.2020.110682

Xamán, J., & Gijón-Rivera, M. (2016). Dinámica de Fluidos Computacional para Ingenieros (Palibrio, Ed.).

Xamán, J., Rodriguez-Ake, A., Zavala-Guillén, I., Hernández-Pérez, I., Arce, J., & Sauceda, D. (2020). Thermal performance analysis of a roof with a PCM-layer under Mexican weather conditions. Renewable Energy, 149, 773–785. https://doi.org/10.1016/j.renene.2019.12.084

Zavala-Guillén, I., Barrera-Román, D., Noh-Pat, F., Sidón, M., García-Pérez, D., & Rodriguez-Ake, A. (2025). Thermal analysis of multi-layered glazed window under Mexican climate. Energy and Buildings, 329, 115259. https://doi.org/10.1016/j.enbuild.2024.115259